IMEKO 2010 TC3, TC5 and TC22 Conferences
Metrology in Modern Context
November 22–25, 2010, Pattaya, Chonburi, Thailand

ANALYSIS OF INDENTER GEOMETRY VERIFICATION DATA BY MEANS OF THE REGRESSION PLANE FITTING

Satoshi Takagi [1], *Tatsuya Ishibashi* [2]

[1] National Metrology Institute of Japan, AIST, Tsukuba, Japan, satoshi.takagi@aist.go.jp
[2] Faculty of Engineering, Niigata University, Niigata, Japan, isibasi@eng.niigata-u.ac.jp

Abstract – An analytical method of the geometrical parameters of hardness indenters from bitmap data obtained AFM, *etc*. is introduced. The method is based on the fitting to the analytical geometric shape by the least square method. The results of the analysis are not influenced by human factors which are usually included in the operation of analyzing software's GUI. Examples of analytical results are shown with the estimation of the uncertainty of measurement. The uncertainty is estimated considering the uncertainty of AFM itself and the misfit of plan regression, and the uncertainty of facet angles, interior angles of the square base of the pyramid and the area function are evaluated for nano-range Vickers indenters through the propagation of error. There are some suggestions that some of the geometrical requirements in ISO 14577 may not practical when the verification process is considered.

Keywords Instrumented indentation, direct verification of indenter, atomic force microscope

1. INTRODUCTION

In these days, several kinds of microscopes such like AFM [1,2,3], confocal microscope, *etc*. have been used for indenter verification especially in micro- to nano-range. These instruments are useful to observe the shape of indenters but it is not always easy to analyze their geometry with their built-in software. Since the data processing with a graphical user interface relies on human eyes and hands, the results must have uncertainty corresponding to human.

In this study, the authors propose a fully mathematical method of analysis, which does not need human operations. Its application to AFM measurement of nano-range Vickers indenter is reported.

2. PROPOSED ANALYTICAL METHOD

2.1. Determination of geometrical parameters

The procedure is developed to analyze bitmap-format surface images obtained with various 3D microscopes. The procedure to analyze geometrical parameters are as follows.

Step 1; the (bitmap) data (Fig. 1 (a)) are divided into three or four groups along the edges of pyramid so that pixels of each plane is contained in each group. Step 2; fit a plane to each pixel group by the least square regression analysis. Now the bitmap data is translated into a model of the analytical geometry, which authors call as the *regression polyhedral model*. Identify the normal of the regression plane as its direction cosine (Fig. 1 (b)). Step 3; define the axis of the pyramid as the composite vector of the normal vectors of all planes (Fig. 1 (c)). Step 4: correct the inclination of the pyramid to the AFM by the rotation of vector (Fig. 1 (d)). It should be noted that the inclination correction is not easy in any other analytical methods although it affects significantly on the analytical results. Step 5; identify facet angles as the relation between the normal vector and the direction vector of the pyramid axis (Fig. 1 (e)). The angle between opposite faces can be determined in similar manner. Step 6; identify the interior angle of the square base of the pyramid (abbreviated to *interior angles*) as the relation of the projected vectors of the normal vectors to *xy* plane (Fig. 1 (f)).

Step 7; determine the length of the line of conjunction (abbreviated to *roof length*) as the distance between two intersection points of regression planes (Fig.1 (g)). In general, the end points of the roof length cannot be seen clearly and it is not easy to determine them exactly. The proposed method can determine these points in fully mathematical process and never include the uncertainty of human eyes.

Step 8; calculate the area functions. The projected area function $A_P(h)$ can be determined by summing up unit areas of pixels from the tip of the pyramid to designated indentation depth, h. If the direction of the pixel is considered, the surface area $A_S(h)$ is obtained (Fig. 1 (h)).

2.2. Estimation of the uncertainty of measurement

The uncertainty of measurement is estimated from two sources. One is the uncertainty of AFM itself and another is the fitting error of the *regression polyhedral model*.

The uncertainty of *x*-, *y*- and *z*-axes of the AFM $u_{image}(x)$, $u_{image}(y)$ and $u_{image}(z)$ are estimated by combining the uncertainty of the reference standard (VLSI STS3-1800P), the resolution of the image, the linearity of the scanner and the effect of the tip radius. It is known that the scanning tip has typically 10-nm radius [4]. The differences of the scanner positions in *x*-, *y*- and *z*-axes between the ideally sharp tip and the typical 10-nm radius tip on the 22° slope (the maximum slope of Vickers pyramid) are, therefore, taken into account.

For further calculation, three components of uncertainty, $u_{image}(x)$, $u_{image}(y)$ and $u_{image}(z)$ should be pooled into one number. In this study, $u_{image}(x)$ and $u_{image}(y)$ are translated to the error of z axis and pooled into newly defined uncertainty $u_{meas,i}(z)$ together with $u_{image}(z)$. The direction of each regression plane is considered in the translation of uncertainty.

An example of the estimation of $u_{image}(x)$, $u_{image}(y)$, $u_{image}(z)$ and $u_{meas,i}(z)$ for a regression plane is shown in Fig. 2. (a).

The standard uncertainty of a regression plane is generally expressed as the root mean square error,

$$E_{\mathrm{RMS},i} = \sqrt{\frac{\{R^2(x_{ij}, y_{ij})\}_j}{N_i - 3}} \tag{1}$$

where $\{R^2(x_{ij}, y_{ij})\}_j$ is the summation of squares of the residuals in the plane i and N_i is the number of pixels consisting plane i.

The standard uncertainty of the coefficients of a regression plane, $(\delta a_i)_{\mathrm{RMS}}$, $(\delta b_i)_{\mathrm{RMS}}$ and $(\delta c_i)_{\mathrm{RMS}}$ can be calculated in conjunction with $E_{\mathrm{RMS},i}$, *i. e.*,

$$\begin{aligned} (\delta a_i)_{\mathrm{RMS}} &= \sqrt{C_{11}} \cdot E_{\mathrm{RMS},i} \\ (\delta b_i)_{\mathrm{RMS}} &= \sqrt{C_{22}} \cdot E_{\mathrm{RMS},i} \\ (\delta c_i)_{\mathrm{RMS}} &= \sqrt{C_{33}} \cdot E_{\mathrm{RMS},i} \end{aligned} \tag{2}$$

where C_{kk} is the component of the inverse tensor of the coefficient tensor of Gauss' normal equation (Fig. 2 (b)).

The uncertainty from two sources, *i. e.*, the AFM and the regression, should be combined into one component so that the uncertainty of every geometrical parameter is estimated through the propagation of errors. The normal sum of square method is used for this operation. An example of the combined uncertainty of a regression plane is shown in Fig. 2. (c).

The uncertainty of facet angles and interior angles can be estimated as shown in Fig. 2. (d).

The uncertainty of the area function is estimated only from $u_{image}(z)$ because $u_{image}(z)$ is the most significant to the area function among all components. The uncertainty and the relative uncertainty are calculated with equations shown in Fig. 2 (e). It should be noted the uncertainty of the area function is calculated with raw data of an AMF image and no curve fitting has done for the area function in the calculation.

3. EXAMPLES OF EXPERIMENTAL RESUTLS AND DISCUSSIONS

In this study, the indenter image was obtained with Pacific Nanotechnology Nano-R AFM, which has a closed loop controlled piezoelectric scanner with positions sensors on it. In *xy* direction, the resolution is < 2 nm (closed loop), the linearity is better than 1 % and in *z* direction, the noise level is < 0.13 nm. The maximum scanning range is 80 µm in *xy* direction and 8 µm in *z* direction [5].

Approximately 5 µm × 5 µm range in the vicinity of the tip of a Vickers indenter for Shimadzu nano-hardness testing machine was observed with the AFM and its geometry was analyzed according to the procedure described in previous section. The results are listed in Table 1. Since the degree of freedom of the uncertainty is typically in the order of 10^8 (for 256 × 256 pixels image), the coverage factor of 1.96 was chosen for 95 % confidence level.

Table 1 Analytiacl results of the geometry of a nano-range Vickers indneter.

Item	Position	Value	Expanded uncertainty†
Facet angle, α	1	68.689°	0.161°
	2	68.509°	0.252°
	3	68.376°	0.246°
	4	67.850°	0.158°
	Average	68.606°	—
Angle between opposite faces, 2α	1 - 3	137.066°	0.294°
	2 - 4	137.360°	0.298°
	Average	137.213°	—
Interior angle of square base, θ	1 - 2	89.332°	2.501°
	2 - 3	91.525°	2.860°
	3 - 4	89.266°	2.424°
	4 - 1	89.876°	1.987°
Roof length, *a*		36.5 nm	—

† Coverage factor of 1.96

As seen in the table, the uncertainty of measurement is larger than requested in ISO 14577-3 (±1.5°)[6]. The uncertainty for the interior angles are much larger than that for the facet angles. This uncertainty is quite sensitive to the inclination of the pyramid axis. According to the simulation, 0.3° of inclination (the maximum permissible error required in ISO 14577-3) can cause 1° of the error of the interior angle even though the indenter has ideal pyramid shape. These results suggest that it is not practical to apply geometrical requirements to micro-range indenters to nano-range indenter and the practical conditions should be discussed under the consideration of verification processes.

The roof usually cannot be seen when it is smaller than 100 – 150 nm. In the proposed method, however, such a small length (in the table) can be identified in the mathematical way.

In Fig. 3, an example of the analyzed area function is demonstrated as the square root of the projected area $A_P(h)$ against the contact depth h. The dots represent the evaluated function from an AFM image while the dashed line represents the curve fit to the equation,

$$A_P(h) = C_0(h + \Delta h)^2 \tag{3}$$

The coefficient C_0 gives the supposition of the facet angles of the pyramid. From the extrapolation of the equation to the point of $A_P(h) = 0$, the truncation length Δh can be estimated. The tip radius is also able to be estimated from C_0 and Δh with the simplified equation [7, 8],

$$r_{eff} = C_0 \cdot \Delta h \text{ (for Vickers pyramid)} \tag{4}$$

when a paraboloid shape is assumed at the tip of the pyramid.

These calculations, however, give the rough characterization of the indenter but not practical to calculate material parameters, *e. g.*, H_{IT} or E_{IT}. One of the reasons is that equation (3) has not enough accuracy especially in the small indentation range and more suitable (accurate but easy to handle) function is expected. In addition, recent study shows that the shape of the rounded area of an indenter tip affects to the elastic behavior of the indenter-material

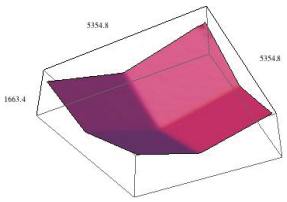

(a) Indenter image ovserved with an AFM.

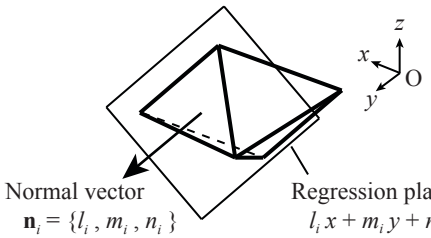

(b) Regression analysis to fit the plane equation.

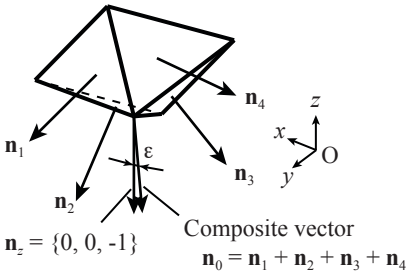

(c) Definition of the pyramid axis.

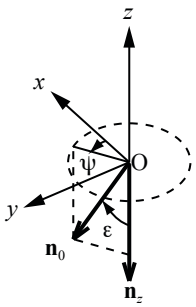

$$\mathbf{P} = \mathbf{T}_z^{-1}(\psi) \cdot \mathbf{T}_y(\varepsilon) \cdot \mathbf{T}_z(\psi) \cdot \mathbf{P}_{meas}$$

(d) Correction of the inclination of axis by vector rotation.

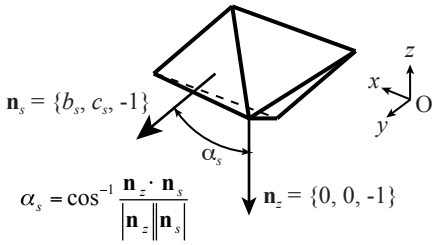

(e) Calculation of facet angles.

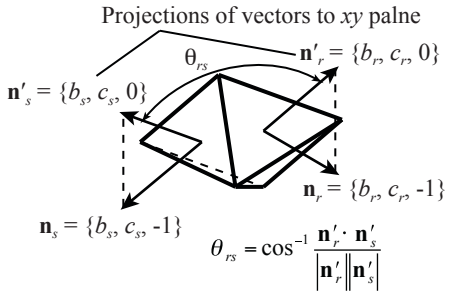

(f) Calculation of interior angles of square base.

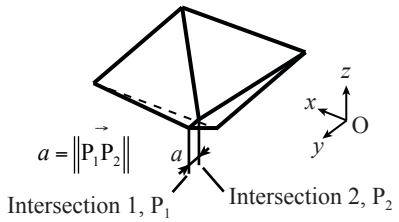

(g) Calculation of the lenght of the line of conjunction.

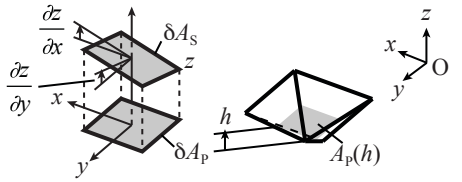

$$A_P(h) = \sum_{i \in R} \delta A_{P,i}$$

$$A_P(h) = \sum_{i \in R} \delta A_{S,i} = \sum_{i \in R} \left[\left\{ 1 + \left(\frac{\partial z}{\partial x} \right)_i^2 \right\} \left\{ 1 + \left(\frac{\partial z}{\partial y} \right)_i^2 \right\} \right]^{\frac{1}{2}} \delta A_{P,i}$$

$$R = \{i, z_i \le h\}$$

(h) Calculation of the area functions (projected and surface).

Fig. 1 Procedure to analyze geometrical characteristics of indenters.

system [9] and the more detailed observation of the indenter tip is also expected.

An example of the estimated uncertainty of measurement for the area function is shown in Fig. 4. It is shown that the uncertainty itself increases with the contact depth *h* but the relative uncertainty is sharply increasing in the small indentation range. It explains how difficult the material characterization in such small range is.

4. CONCLUSIONS

A method to analyze indenter geometry verification data, which is based on the regression plane fitting and analytical geometry of the planes, is introduced. By applying the method to the analyses of indenter verification data, From the application of the method, it was shown that geometrical

(a) Uncertainty of the AFM.

$u_{image}(x)$, $u_{image}(y)$, $u_{image}(z)$ are the combination of, the uncertainty of the reference standard, resolution, linearity and the effect of the tip radius.

Pooling $u_{image}(x)$, $u_{image}(y)$ and $u_{image}(z)$ into $u_{meas,i}(z)$.

$$u_{meas,i}(z) = \left[\left(\frac{\partial z}{\partial x}\right)^2 \cdot u_{image}^2(x) + \left(\frac{\partial z}{\partial y}\right)^2 \cdot u_{image}^2(y) + u_{image}^2(z)\right]^{\frac{1}{2}}$$

$$= \left[b_i^2 \cdot u_{image}^2(x) + c_i^2 \cdot u_{image}^2(y) + u_{image}^2(z)\right]^{\frac{1}{2}}$$

Table i. Estimated uncertainty of the AFM.

Component	Symbol	Standard uncertainty, nm
x-axis	$u_{image}(x)$	} 54.9
y-axis	$u_{image}(y)$	
z-axis	$u_{image}(z)$	7.92
Pooled	$u_{meas,i}(z)$	471.9

(b) Uncertainty of the regression planes.

Table ii. An example of the uncertainty estimation of a regression plane

Component	Symbol	Standard uncertainty
Regression	$E_{\mathrm{RMS},i}$	3.8 nm
a_i	$(\delta a_i)_{\mathrm{RMS}}$	0.25 nm
b_i	$(\delta b_i)_{\mathrm{RMS}}$	0.00082
c_i	$(\delta c_i)_{\mathrm{RMS}}$	0.00094

(c) Combination of the uncertainty of the AFM and the regression.

$$E^*_{\mathrm{RMS},i} = \left(E^2_{\mathrm{RMS},i} + u^2_{meas,i}(z)\right)^{\frac{1}{2}},\ (\delta a_i)^*_{\mathrm{RMS}} = \sqrt{C_{22}} \cdot E^*_{\mathrm{RMS},i},\ \ldots$$

Table iii. An example of the combined uncertainty of a regression plane

Component	Symbol	Standard uncertainty
Regression	$E^*_{\mathrm{RMS},i}$	471.9 nm
a_i	$(\delta a_i)^*_{\mathrm{RMS}}$	30.2 nm
b_i	$(\delta b_i)^*_{\mathrm{RMS}}$	0.10
c_i	$(\delta c_i)^*_{\mathrm{RMS}}$	0.12

(d) Calculation of the uncertainty of facet angles α_s and the interior angle of the square base θ_{rs} by the propagation of error.

$$u^2(\alpha_s) = \left(\frac{\partial \alpha_s}{\partial b_s}\right) \cdot (\delta b_s)^{*2}_{\mathrm{RMS}} + \left(\frac{\partial \alpha_s}{\partial c_s}\right) \cdot (\delta c_s)^{*2}_{\mathrm{RMS}}$$

$$u^2(\theta_{rs}) = \left(\frac{\partial \theta_{rs}}{\partial b_r}\right) \cdot (\delta b_r)^{*2}_{\mathrm{RMS}} + \left(\frac{\partial \theta_{rs}}{\partial c_r}\right) \cdot (\delta c_r)^{*2}_{\mathrm{RMS}}$$

$$+ \left(\frac{\partial \theta_{rs}}{\partial b_s}\right) \cdot (\delta b_s)^{*2}_{\mathrm{RMS}} + \left(\frac{\partial \theta_{rs}}{\partial c_s}\right) \cdot (\delta c_s)^{*2}_{\mathrm{RMS}}$$

(e) Uncertainty estimation of the area function. It is based on the fact that the error in z-axis is dominant to that in other axes.

$$u(A) = \frac{\partial A}{\partial h} \cdot u_{image}(z)$$

$$u_{rel}(A) = \frac{u(A)}{A(h)}$$

Fig. 2 Procedure to estimate the uncertainty of measurement.

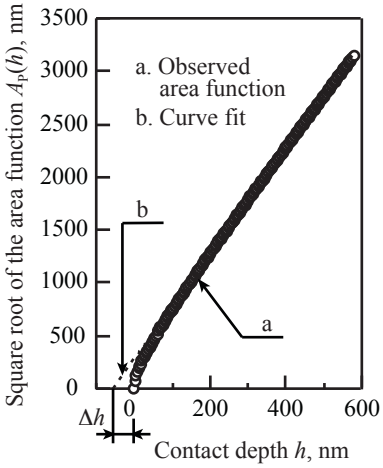

Fig. 3 An example of the evaluated area function.

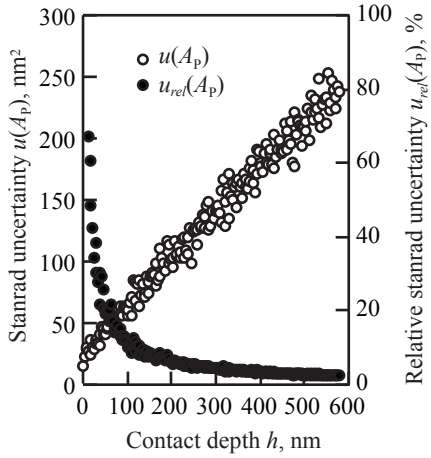

Fig. 4 An example of the uncertainty of measurement of the area function.

parameters were evaluated for a Vickers indenter as well as the uncertainty of measurement. the method can eliminate human factor on the uncertainty of measurement and determine geometrical parameters fully mathematical way, and that the uncertainty of interior angles are quite sensitive to the inclination of the pyramid axis. The example suggests that the geometrical requirements in current ISO 14577 for nano-range indenters should be considered.

REFERENCES

[1] K. Hasche, K. Herrmann, F. Pohlenz and K. Thiele, *Meas. Sci. Technol.*, **9** (1998) 1082-1086.

[2] S. Takagi, T. Usuda, R. Kongkavitool, T. Ishibashi, *J. Mater. Test. Res. Assoc. Jpn.*, **52**, 3 (2007) 169-175.

[3] A. C. Fischer-Cripps, *J. Mater. Res.* **25** (2010), 927-934.

[4] PointProbe® Plus, NANOSENSORS™ product catalog.

[5] Nano-R™, AFM User's Manual, Pacific Nanotechnology, Inc. (2002)

[6] ISO 14577-3: 2002.

[7[Y. Murakami, K. Tanaka, M. Itokazu, A. Shimamoto, *Phil. Mag.* A, **69**, 6 (1994) 1131-1153.

[8] A. Shimanoto, K. Tanaka, Y. Akiyama, H. Yoshizaki, *Phil. Mag.* A, **74**, 5 (1996) 1097-1105.

[9] Y. Yoshikawa, T. Ishibashi, S. Katayama, M. Ohki, S. Takagi, *J. Mat. Test. Res. Assoc. Jpn*, **53**, 2 (2008) 149-155.